SEECCM III
3rd South-East European Conference on Computational Mechanics-
an ECCOMAS and IACM Special Interest Conference
M. Papadrakakis, M. Kojic, I. Tuncer (eds.)
Kos Island, Greece, 12–14 June 2013

ENDLESSLY TOUCHABLE – THE NEXT GENERATION OF SURFACE AND COATING OPTIMIZATION

ABOUT THE IDENTIFICATION OF GENERIC TRIBOLOGICAL PARAMETERS, SOPHISTICATED COMPLETELY ANALYTICAL CONTACT MODELING AND THE EFFECTIVE INDENTER CONCEPT APPLIED TO A COMPREHENSIVE 3D INCREMENTAL WEAR AND FRETTING MODEL FOR LAYERED SURFACES

Norbert Schwarzer[1]

[1] Saxonian Institute of Surface Mechanics SIO
Tankow 2, 18569 Ummanz / Rügen,
Germany, www.siomec.de

e-mail: n.schwarzer@siomec.de

Keywords: Tribology, contact problems, nanoindentation, scratch, wear, extended Hertzian

Abstract. *To obtain tribological parameters like Archard's wear depth parameter kd usually requires some severe effort in performing and analyzing complex tribological experiments. The paper features an approach where such parameters are extracted from effective interaction potentials [1], which themselves are built up and fed from more physical-oriented measurements like Nanoindentation and PHYSICAL scratch. By using such effective material potentials one can derive critical loading situations leading to failure (decomposition strength) for any contact situation. A subsequent connection of these decomposition or failure states with the corresponding stress or strain distributions allows the development of rather comprehensive tribological parameter models applicable in wear and fatigue simulations as demonstrated in this work.*

From this a new sophisticated wear model has been developed on the basis of the effective indenter concept [1, 2] by using the extended Hertzian approach [3, 4]. The models do not only allow to analyze certain tribological experiments like the well known pin-on disk test or the more recently developed nano-fretting tests, but also to forward simulate such tests and even give hints for better component life-time predictions. The work will show how the procedure in principle is to be applied and a few examples will be presented in the corresponding talk.

Introduction

In order to achieve the goal set in the headline, namely, the extraction of generic tribological or wear parameters it is necessary to combine quite a few fields and/or concepts of material science. Therefore this introduction needs to cover the following issues:

- first principle based interatomic potential description of mechanical material behavior
- the effective indenter concept
- the extension of the Oliver and Pharr method to analyze nanoindentation data to layered materials and time dependent mechanical behavior
- the physical scratch and/or tribological test and its analysis

Simple first principle based interatomic potential description of mechanical material behavior

It was shown in [5] that on the basis of an effective potential function like the Morse potential given as

$$V_{Morse} = \varepsilon\left[e^{-2p(r-r_0)} - 2e^{-p(r-r_0)}\right] \qquad (1)$$

a contact problem can be evaluated using the mechanical parameters derived from such a potential. Here p, ε, σ are material parameters and r_0 usually denotes the equilibrium bond length. In such a case the potential would define the pair interaction. Here however, as in [1, 5], we will apply the potential as an effective one with r_0 denoting the lattice constant (see also [6]). With respect to molecular dynamic simulation such an effective potential could be the basis for the extraction of the necessary pair and higher order interactions as demonstrated in [6]. For our study however, we will not need this, because we are only interested in the mechanical constants, especially the Young's modulus and the decomposition strength. Having this, one can apply the method described in [5] to simulate a mechanical contact problem, thereby even taking nonlinear effects like the pressure dependency of the Young's modulus into account.

Brief story about the "effective indenter concept" and its extension to layered materials

Surface usually is not bulk and so, subsequently the behavior of surfaces, especially their mechanical behavior can be dramatically different from what one might expect by just applying bulk concepts to surface problems like contact situations with very surface-located, surface-dominated stress and strain fields. In tribo and wear problems this very often compromises our ability to simulate and understand the physical processes taking place in certain tests (e.g. [7 - 11]). In order to improve this situation we therefore resort to a stringent application of a layered material model considering and modeling the mechanical surface always as - at least potentially - having a property profile starting from the mechanical bulk values in depth usually well known for a certain material to rather often completely different properties on the top-most surface layer. In the case of coated materials this model extension, of course, can easily be justified by the explicit coating structure. However, we should stress the point of also carefully and critically considering apparent "homogenous surfaces" as - rather often - being of gradient or somehow layered character.

The "effective indenter concept" itself can mathematically be described or understood as some kind of quasi conform coordinate transformation transforming the difficult problem of a curved surface contacted by a well defined indenter (like a cone) into a flat surface loaded with a complexly formed indenter. Already in 1995 Bolshakov, Oiver and Pharr [12] introduced this “Concept of the Effective Indenter” and refined it in a series of wonderful publica-

tions until in 2002 the paper about "Understanding of nanoindentation unloading curves" [13] was published by Pharr and Bolshakov.
The extension of this concept is simply performed by substituting the homogenous half space model describing the loaded sample body by a layered half space model [14].

Brief description of the extension of the Oliver and Pharr method to analyze nanoindentation data to layered materials and time dependent mechanical behavior

As it is a well established fact, that the classical Oliver and Pharr method [15], as an approach based upon the homogenous half space model, cannot directly be applied to layered materials and small structures, the author here refers to the literature [e.g. 16]. Soon after the publication of the Oliver and Pharr method it became clear that there is a physical concept this method can be based on which was called the "Concept of the Effective Indenter" [13, 14]. During a small conference in Italy in 1999, the author learned of that concept and decided to work out a theory solving not only the problem for the mechanical contact of an indenter with general shape of symmetry of revolution, but also to extend this solution to layered structures. He published its solution in 2004 [17]. Later on he also presented a variety of applications together with Pharr, Chudoba, Richter and others [18 - 23]. As a rather stubborn theoretician however, the author needed some motivation from most of the authors mentioned above, especially Pharr, before he realized that the "effective indenter theory", even though powerful, was not something one could easily give to the engineer or an indenter experimentalist and expect him to use it as a tool for the analysis of indentation data. The reason for this is the complexity of the formulae building up the solution. Thus, the whole approach was brought into a software package named FilmDoctor® [24].

Making the classical Oliver and Pharr method fit for time dependent mechanical behavior

In an indentation test we always find complex 3-dimensional stress states with usually all stress components being non-zero. Thus, as Fischer-Cripps put it "the nature of the loading is a complex mixture of hydrostatic compression, tension, and shear" [25]. In the case of viscous behavior we also have to understand that we even have complex mixtures of stress and strain rates. These however, usually influence the time dependent mechanical parameters [26]. This automatically means that at different positions we find different stress and strain states and rates leading to different mechanical parameters (time dependent) at different positions within the material. This automatically makes the system of linear partial differential equations of linear Elasticity non-linear in the moment viscosity (even elastic viscosity) comes into play. In order to keep things simple however, we will not go here for a non-linear basic solution, but try to find effective, phenomenological descriptions for visco-elastic, visco-plastic contact problems based on the concept of a time dependent effective indenter.

Introduction into the physical scratch and/or tribological test and its analysis

The standard scratch test is a widely used method to test the mechanical stability of coatings on different types of substrates and has become a sensitive technique to control the reliability of the manufacturing process. It is based on various standards [27, 28].
Since the part above covered the calculation of true mechanical layered surface properties by nanoindentation, all mechanical values are known which are not only required to properly dimension (fine-tune) a scratch or tribology test for specific surface structures, but also is of need for a physical analysis of these tests. The following flow chart might give an illustrative understanding into such a test procedure.

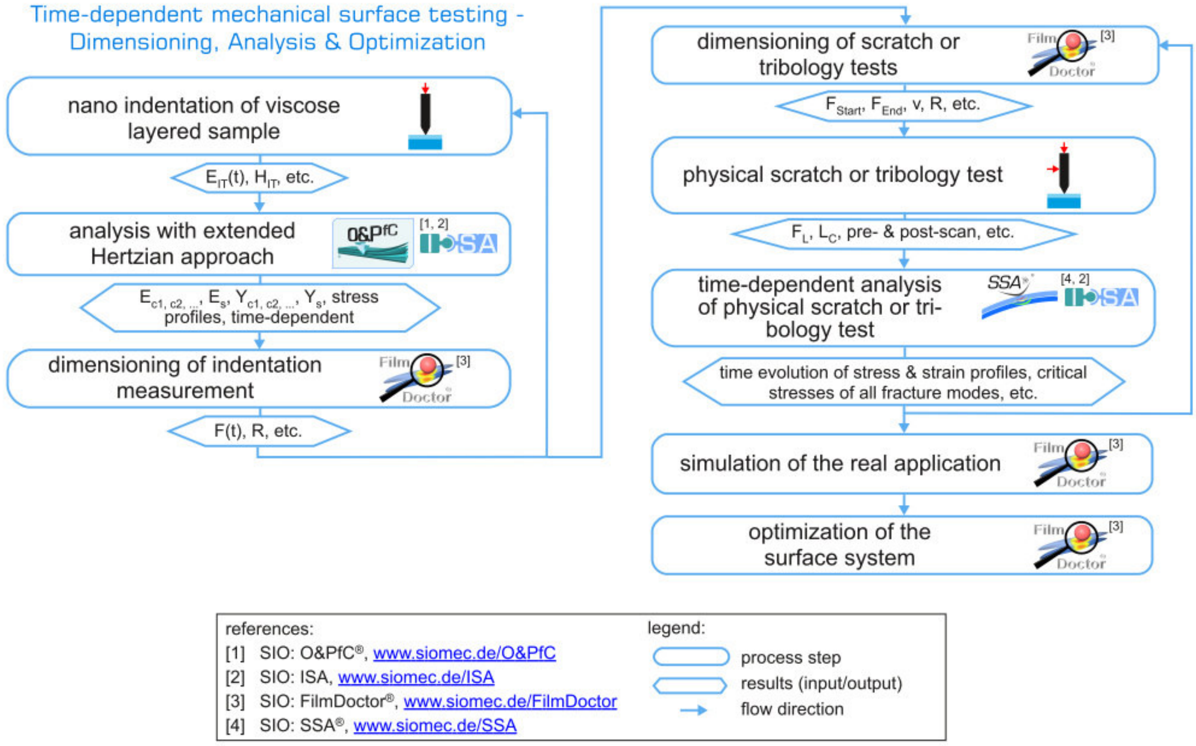

Fig. 1: A flow chart of the procedure of mechanical characterization and optimization of arbitrary structured surfaces with possibly time dependent mechanical properties

The reader will find illustrative examples and a much more comprehensive elaboration of the method in [29] and [30].

Theory

First principle based interatomic potential description of mechanical material behavior

As shown in [1] the pressure P and bulk modulus B can be derived from an effective potential. Thereby it is convenient to express P and B in units of B_0 (B at P=0) and by substituting the lattice distance r by $r=c*r_0$ result in the relations:

$$P/B_0=\frac{e^{r_0 p(1-c)}}{r_0 p c^2}\left[1-e^{r_0 p(1-c)}\right];\quad B/B_0=\frac{e^{r_0 p(1-c)}}{r_0 p c^2}\left[2\left(1+r_0 p c\right)e^{r_0 p(1-c)}-2-r_0 p c\right] \qquad (2)$$

We also take as estimates for the critical r leading to decomposition (c.f. [1]) the following expressions which have to be solved numerically ($r_{00} = p*r_0$):

$$6\left(1+c_m r_{00}\right)-3e^{r_{00}\left(c_m-1\right)}\left(2+c_m r_{00}\right)=0 \qquad (3)$$

to extract the critical c-value c_m for maximum P(c).

As a purely mathematically based measure for the critical bond length or in our case of an effective potential the lattice distance, the inflexion point for $c_{ifp}>c_m$ could be used. This can be numerically obtained for the Morse potential via:

$$6+c_{ifp} r_{00}\left(4+c_{ifp} r_{00}\right)-2e^{r_{00}\left(1-c_{ifp}\right)}\left(3+2c_{ifp} r_{00}\left(2+c_{ifp} r_{00}\right)\right)=0 \qquad (4)$$

The effective indenter concept

In order to have a sufficiently great variability for the definition of differently shaped "effective indenters", we apply the extended Hertzian approach as shown for example in [31]. With this approach normal and even tangential load distributions of the form [17]

$$\sigma_{zz0}(r,\varphi)=\sum_{n=0}^{N}c_{\sigma n}r^{n}\sqrt{a^{2}-r^{2}} \tag{5}$$

$$\begin{aligned}\tau_{rz0}(r,\varphi)&=\sum_{n=0}^{N}c_{\tau rn}r^{n}\sqrt{a^{2}-r^{2}}\\ \tau_{xz0}(r,\varphi)&=\sum_{n=0}^{N}c_{\tau xn}r^{n}\sqrt{a^{2}-r^{2}}\\ \tau_{yz0}(r,\varphi)&=\sum_{n=0}^{N}c_{\tau yn}r^{n}\sqrt{a^{2}-r^{2}}\end{aligned} \tag{6}$$

with n=0,2,4,6 and arbitrary constants c (and by following the instructions of the mathematical procedures for obtaining the complete potential functions as given in [17] even arbitrary high but only even N) can be solved completely.

Together with lateral loads (occurring in all scratch- and tribotesters or the next generation of nanoindenters and their applications, see e.g. [31, 33, 34]) one often faces tilting moments leading to a normal surface stress distribution of the form

$$\sigma_{zz0}(r,\varphi)=\sum_{n=0}^{N}c_{\sigma n}r^{n+1}\cos(\varphi)\sqrt{a^{2}-r^{2}}\ . \tag{7}$$

These stresses can for example occur when the indenter shaft is dragged over the surface. Because the shaft itself is elastic and thus would be bent during the lateral loading, an unavoidable tilting moment results and acts on the contacted surface. Also curved surfaces (e.g. due to roughness) can lead to such tilting moments.

A defect model: Tool for the construction of relatively general intrinsic stress distributions caused by internal inhomogeneities

In order to simulate the internal complex material structure of porous or composite materials, certain defect fields must be developed and combined with the external loads. Circular disc-like inclusions could for example be simulated by the use of plane defects within the layered half space. So, introducing circular defects of radii a_i of the loading type:

$$\begin{aligned}\tau_{rz0}\left(r_i=\sqrt{(x-x_i)^2+(y-y_i)^2},z_i+0\right)&=\sum_{n=0}^{N}c_{\tau i,n}r_i^{n}\sqrt{a_i^{2}-r_i^{2}}\\ \tau_{rz0}\left(r_i=\sqrt{(x-x_i)^2+(y-y_i)^2},z_i-0\right)&=-\sum_{n=0}^{N}c_{\tau i,n}r_i^{n}\sqrt{a_i^{2}-r_i^{2}}\end{aligned} \tag{8}$$

$$\begin{aligned}\sigma_{zz0}\left(r_i=\sqrt{(x-x_i)^2+(y-y_i)^2},z_i+0\right)&=\sum_{n=0}^{N}c_{\sigma i,n}r_i^{n}\sqrt{a_i^{2}-r_i^{2}}\\ \sigma_{zz0}\left(r_i=\sqrt{(x-x_i)^2+(y-y_i)^2},z_i-0\right)&=-\sum_{n=0}^{N}c_{\sigma i,n}r_i^{n}\sqrt{a_i^{2}-r_i^{2}}\end{aligned}\ . \tag{9}$$

(with x_i, y_i, z_i denoting the centre of the defect and n=0,2,4,6) directly allows us the application of the extended Hertzian approach [17] that provides a complete solution of the elastic field of the defect loading given above. By superposing a multitude of such "defect dots", one could model (simulate) a very great variety of material inhomogeneities and intrinsic stress distributions. The evaluation of the complete elastic field is straight forward. It only requires the evaluation of certain derivatives of the potential functions given in [17].
Finally, we need to take into account the curvature of the surfaces in order to its effect on the resulting contact pressure distribution [32]. As the theoretical approach would not find enough space in this short note, the author will publish the necessary details elsewhere. However, the interested reader may derive the results presented here by comparing the solutions of the Laplace equation in Cartesian and Paraboloidal coordinates.

The extension of the Oliver and Pharr method to analyze nanoindentation data to layered materials and time dependent mechanical behavior

Oliver and Pharr [15] have shown that the force removal curve from elasto-plastic deformations with a Berkovich indenter can be described by a power function:

$$F = C \cdot (h - h_0)^m \qquad (10)$$

Applying now the concept of the effective indenter as shown in fig. 2 one can easily deduce that such an unloading curve can be connected with an Indenter of the shape.

$$Z(r) = B \cdot r^n , \qquad (11)$$

with:

$$\begin{aligned} m &= 1 + \frac{1}{n} \\ C &= 2 \cdot E_r \cdot \left[\frac{n}{n+1}\right] \cdot \left(\frac{1}{B} \cdot \left[1 - \varepsilon \cdot \frac{n}{n+1}\right]\right)^{\frac{1}{n}} \\ \frac{1}{E_r} &= \frac{1-\nu_i^2}{E_i} + \frac{1-\nu_s^2}{E_s} \\ \varepsilon &= m \cdot \left[1 - \frac{1}{\sqrt{\pi}} \frac{\Gamma\left(\frac{m}{2 \cdot m - 2}\right)}{\Gamma\left(\frac{2 \cdot m - 1}{2 \cdot m - 2}\right)}\right] \end{aligned} \qquad (12)$$

The indices i and s are standing for the indenter and sample, respectively.

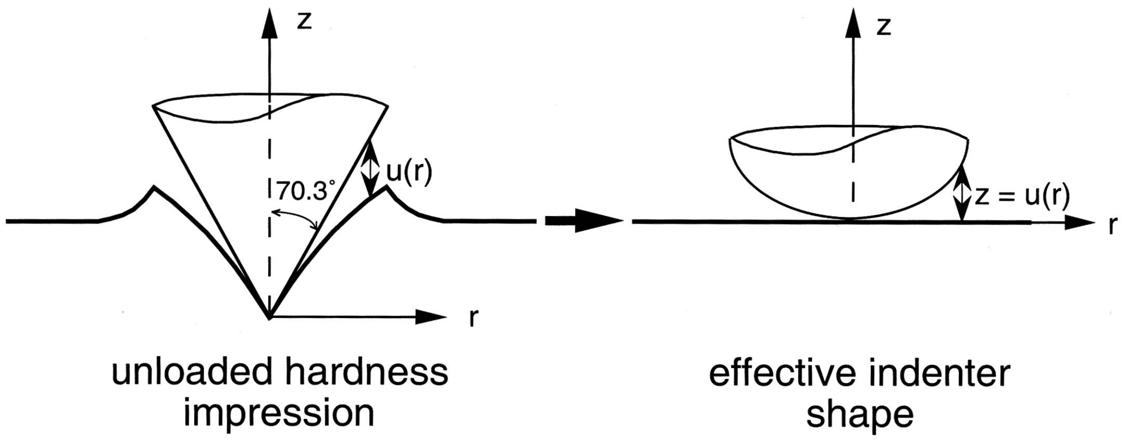

Fig. 2: The effective indenter concept (see: G. M. Pharr, A. Bolshakov: J. Mater. Res., Vol. 17, No. 10, Oct 2002) transferring the theoretical difficult problem of a well defined sharp indenter on a elasto-plastically deformed surface with complex shape (left hand side) by an effective indenter on a flat surface.

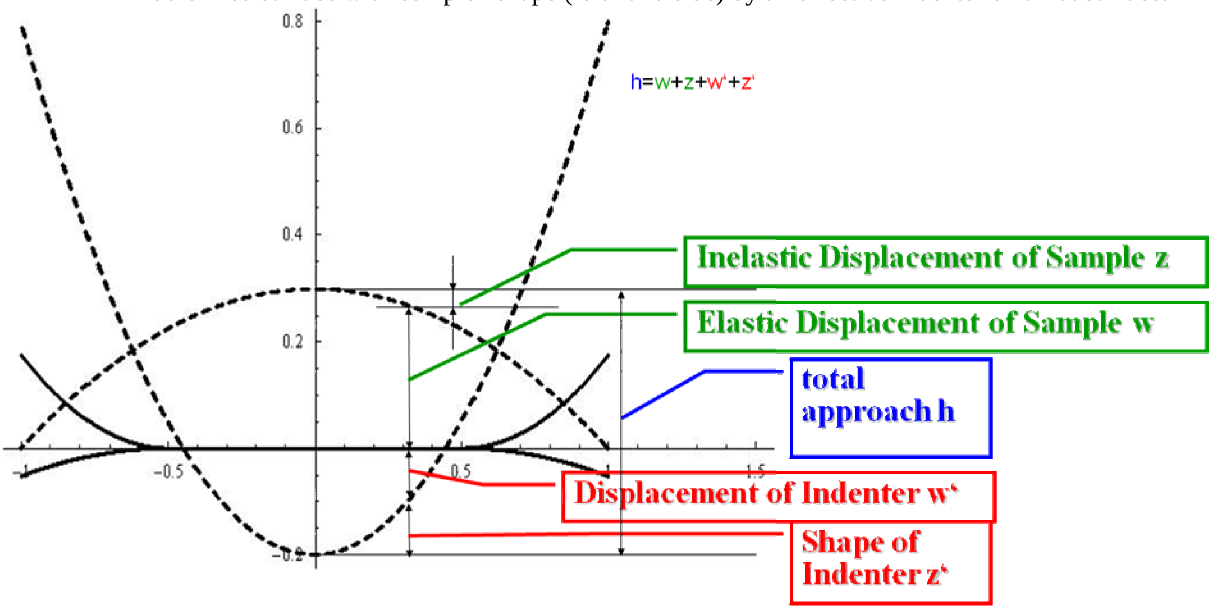

Fig. 3: Formulating the contact equation h=w+z+w'+z' with respect to partial plastic deformation z of the sample surface

For this one needs to reformulate the basic contact equation incorporating the plastically deformed surface of the sample with the locally defined shape function (fig. 3)

$$z(r) = B_S \cdot r^n , \tag{13}$$

Together with the following approach for the indenter part being in contact with the sample surface of the kind

$$z'(r) = B_I \cdot r^n , \tag{14}$$

we obtain

$$w(r) + w'(r) = h - (B_I + B_S) \cdot r^n , \tag{15}$$

as the new governing contact equation with the parameters $B=B_I+B_S$ and n defining the effective indenter shape Z(r), as given above.

Similarly also more general effective indenter concepts can be derived, like this one

$$\begin{aligned} w_S(r)+w_I(r) &= h-\frac{r^2}{d_0}-\frac{r^4}{d_2}-\frac{r^6}{d_4}-\frac{r^8}{d_6} \\ &= h-r^2\left(\frac{1}{d_0^{Indenter}}-\frac{1}{d_0^{plastic\ shape}}\right)-r^4\left(\frac{1}{d_2^{Indenter}}-\frac{1}{d_2^{plastic\ shape}}\right), \\ &-r^6\left(\frac{1}{d_4^{Indenter}}-\frac{1}{d_4^{plastic\ shape}}\right)-r^8\left(\frac{1}{d_6^{Indenter}}-\frac{1}{d_6^{plastic\ shape}}\right) \\ &= h-r^2\left(c'_0-c_0\right)-r^4\left(c'_2-c_2\right)-r^6\left(c'_4-c_4\right)-r^8\left(c'_6-c_6\right) \end{aligned} \tag{16}$$

based on a locally paraboloid surface with r-terms r^0, r^2, r^4, r^6 and r^8. The reader might easily recognize the extended Hertzian character [22] of the basic contact equation given above as the more simpler Hertzian contact would read:

$$\begin{aligned} w_S(r)+w_I(r) &= h-\frac{r^2}{d_0} \\ &= h-r^2\left(\frac{1}{d_0^{Indenter}}-\frac{1}{d_0^{plastic\ shape}}\right), \\ &= h-r^2\left(c'_0-c_0\right) \end{aligned} \tag{17}$$

Some of the following examples and discussions will be based on these more general approaches. However, due to the wide use of the power law fit given above we will explicitly concentrate on the practical examples being performed using the power law approach.
In [17] and [22] it is shown how these general contact approaches can be applied and how the complete elastic fields have to be evaluated while the extension to the case of layered materials is been elaborated in [14]. Extension to tilting and lateral loads is given in [22] and [24].
The next thing of need now is a time dependent analysis method for ordinary quasi-static nanoindentation tests (e.g. [35] with application [36]). Our approach will be of the following kind [25]:

$$F=C*(h-h_0)^m \quad \to \quad F=C(t)*(h-h_0(t))^{m(t)} \tag{18}$$

with t denoting the time.
The next step is the introduction of a time dependent material model. Here we resort to the well known three parameter approach given by a Young's modulus of the following kind $E(t)=E_0+E_1 \mathrm{Exp}[-t/\tau_R]$ ($\tau_R \equiv \tau$... relaxation time).
Now we substitute the time dependent Young's modulus into the function C(t) of equation (18) and obtain

$$F=2\cdot\left(\frac{1-\nu_i^2}{E_i}+\frac{1-\nu_s^2}{E_{s0}+E_{s1}\cdot e^{-\frac{t}{\tau}}}\right)^{-1}\cdot\left[\frac{n}{n+1}\right]\cdot\left(\frac{1}{B}\cdot\left[1-\varepsilon(n)\cdot\frac{n}{n+1}\right]\right)^{\frac{1}{n}}*(h-h_0)^{\left(1+\frac{1}{n}\right)} \tag{19}$$

This makes the classical fit of the three constants h_0, m and C a time dependent 6-parameter fit of h_0, n, B and the material constants E_0, E_1 and τ_R. It is clear that so many parameters in just one curve will automatically lead to numerical difficulties and instabilities. Thus, even in the pure visco-plastic case it is strongly suggested to use a variety of curves (3 might be good number) obtained with different unloading speeds or at different maximum loads with similar unloading times.

In cases of time dependent inelastic behavior (like visco-plasticity) or more complex constitutive laws also n, B and h_0 have to be taken as n(t), B(t), $h_0(t)$ making the fit even more complex. The same holds in the visco-elastic case for just h_0 when there are great differences between unloading time and τ_R (comparable strain rates). The parameters n and B on the other hand are then only geometrical parameters and do not explicitly depend on time.
A more detailed derivation and discussion of this extension is to be found in [37].

Theory for the physical scratch and/or tribological test

The governing contact equation and stress distributions for more general loading condition as occurring during tests like scratch and pin on disc have already been given in the section "the effective indenter concept". The evaluation of the complex stress and strain fields for these tests is elaborated in the references given there. However, as these evaluations are rather cumbersome and lengthy, the reader is also referred to a software package performing such calculations in an automated and quick manner [24].
It should explicitly pointed out here, that knowledge of the complete stress and strain field is essential for a proper failure characterization (scratch) or wear mechanism analysis (tribo). An example is presented in the figures below.

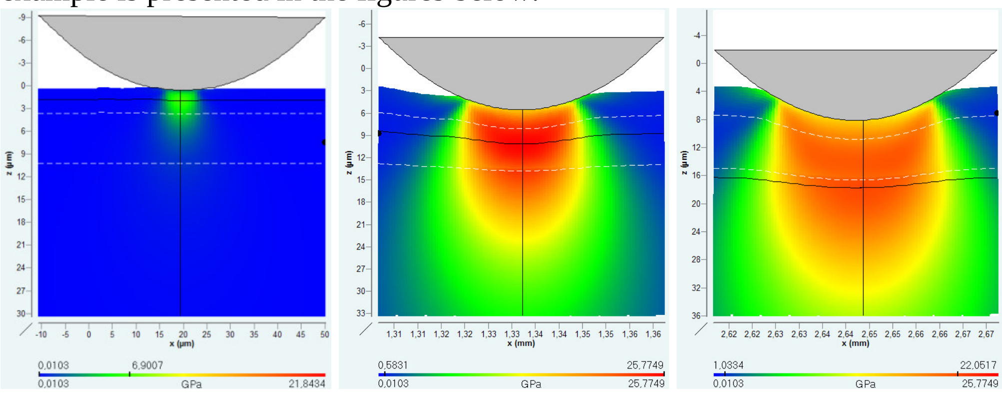

Fig. 4: The evolution of von-Mises stress during the scratch test shown at three measurement points: (a) at the beginning of the scratch test, (c) in the moment of LC failure, and (b) in between. The black cross hairs indicate the location of the maximum.

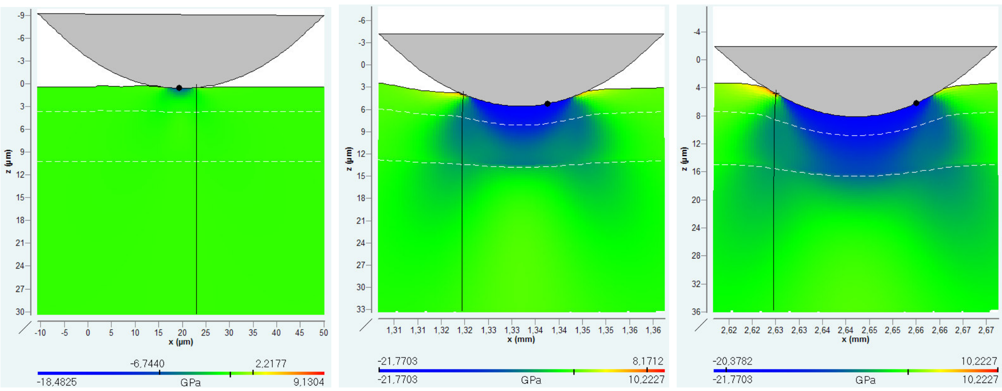

Fig. 5: The evolution of normal stress in scratch direction illustrated at three measurement points: (a) at the beginning of the scratch test, (c) in the moment of LC failure, and (b) in between. The black coss hairs indicate the location of maximum tensile stress.

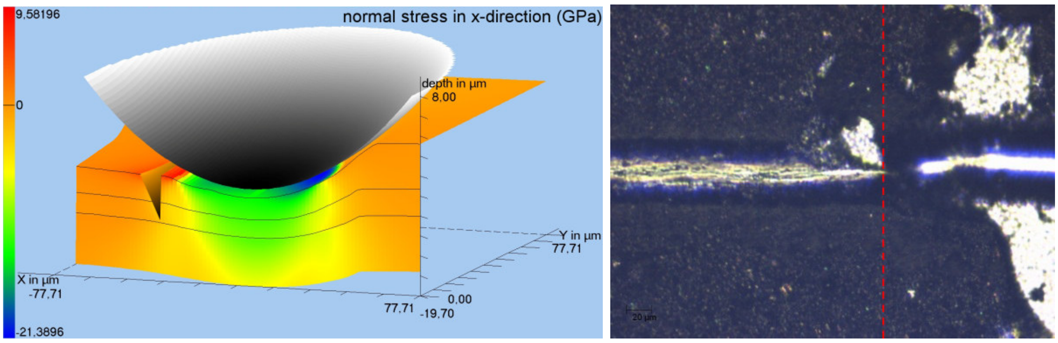

Fig. 6: Illustrative scheme of the failure mechanism (a) and an optical graph of the post-scratch surface (b) in which the corresponding LC position is marked by the red dashed line.

Hence, only such a physical analysis of mechanical contact measurements like instrumented indentations, scratch and tribo-tests enables one to find out why a surface structure fails under certain loading conditions. These results provide indications on how the investigated coating structure can be improved.

From quasi-static experiments and parameters to dynamic wear, fretting and tribological tests

Now we need to establish the relationship between quasi-static characteristics, like hardness, yield strength, Young's modulus etc. etc. and highly dynamic characteristics like wear, fretting and other tribological processes and effects.
First of all, it must be understood that within the concept of this approach the process of wear, fretting or general tribological process is a to be considered as a multi-physical multi body (asperity) ensemble of contact situation (called load dots, c.f. [40]) with each having its own geometry, load conditions (including tilting, normal, lateral, twisting loads plus frictional caused temperature fields) and – in complex cases with debris – also multiple time scales, meaning varies parts of the global tribological contact are running in their own speed. Of course, we will then have to take temperature effects often coupling back into the mechanical properties and time dependent material behavior (c.f. section "The extension of the Oliver and Pharr method to analyze nanoindentation data to layered materials and time dependent mechanical behavior") into account. However, the mathematics of partial differential equations does provide an interesting short cut here. It is due to the similarity of the governing differential equations that having found the solution for the contact problem immediately gives us the solution for the temperature field or any other "diffusion-like" problem. So, the layered solution for any diffusion problem can be extracted from the elastic solution by letting the Poisson's ratio go to infinity leading to perfectly non-singular field solution for the diffusion problem in question.
Beside that: The connection between non-physical parameters (like hardness) towards wear is not the intention of the paper. In fact, there is no such connection – strictly speaking. Something not generic like hardness simply cannot – not generally – be extended or applied to a dynamic process like wear. To put it metaphorically: Somebody who intends to model the gravity and curvature of space around a very dense star will probably not try to start with Galilei´s fall experiments and concepts but uses the Einstein field equations instead.
Where is the role of debris particles?
They are just adding up to the complex jumble of contact situations mentioned above.
How are strain rate effects taken into account?
By applying either piecewise 3-parameter models or solving the nonlinear governing system of equations with time-stress- and strain-dependent material parameters (c.f. section "The extension of the Oliver and Pharr method to analyze nanoindentation data to layered materials and time dependent mechanical behavior").

How are intrinsic stress been taken into account?
Intrinsic stresses are just adding to the external stresses (and strain) fields and lead to a subsequent shift of onset of inelastic behavior, be it fracture, plastic flow or phase transition. Therefore it is very important to know and consider intrinsic stresses as accurately as possible. Here "accurately" explicitly means that intrinsic stresses are usually not homogeneously distributed but also present a complex field adding up to the deformation field coming from external loading situations.
How is the wear of the system (both the softer and harder of the materials) accounted for?
By decomposition limits extracted from the first principle approaches as described in the procedure-plan below. The concepts of "softer" or "harder" have nothing to do with this general approach.
How can this be achieved in a rather general manner?

The most general way would be to extract decomposition limits from the first principle approaches as described in [2]. These limits have then to be compared with the deformation fields obtained in the multiple complex contact model describing our tribo, fretting or wear experiments. Thereby, we explicitly point out, that wear cannot be connected by a simple k_d-value (simple Archard's law) to the deformation or stress field. Instead, in the most simple and linear case, the tribo-effect is a tensor, coupling with wear-moduli to every deformation field component in a fully covariant manner. More correctly any tribo-process could be linearly generalized like:

$$tribo-effect_{ij} = k^{\sigma}{}_{ijkl}\ \sigma^{kl} + k^{\varepsilon}{}_{ijkl}\ \varepsilon^{kl} + k^{u}{}_{ijkl}\ u^k u^l + \sum_{n=1}^{N} k^{S_n} \delta_{ij} S_n \tag{20}$$

Here we used the following denotations: $k^{xx}{}_{ijkl}$-tensors are tensors coupling to the various field values or tensors like the stress σ^{kl}, strain ε^{kl}, displacement-vector u^i or scalar values S_n, like free or distortion energy strain work etc.. The symbol δ_{ij} is the Kroenecker symbol. In most cases, wear for instance, it should be sufficient to consider only the stresses:

$$tribo-effect_{ij} \equiv w_{ij} = k_{ijkl}\ \sigma^{kl} \tag{21}$$

Wherefrom the scalar wear-depth h_w has to be evaluated via:

$$h_w = w_{ij}\ n^i\ n^j \tag{22}$$

With n^i denoting the surface normal unit vector.
As we can see, the Archard's law given with a scalar wear coefficient k_d by the simple relation $h_w=k_d * \sigma^{33}$ is nothing but a rather dramatic simplification of equation (21) being possible wherever either the stress is dominated by its normal component in the surface normal direction (here we named it σ^{33}) or where the coefficient tensor k_{ijkl} is zero except for those components coupling to the normal surface stress σ^{33}, which would then read:

$$h_w = w_{ij}\ n^i\ n^j = k_{ijkl}\ \sigma^{kl} n^i\ n^j = k_{33kl}\ \sigma^{kl} \simeq k_{3333}\sigma^{33} \equiv k_d \sigma^{33} \tag{23}$$

We can deduce now that for complex contact conditions, where the stress tensor is fully set and no component is dominant against all the others one should be rather careful with the assumption of having the wear-tensor being of the most simple, Archard's-law-like kind

$k_{33kl} = \begin{pmatrix} 0 & 0 & 0 \\ 0 & 0 & 0 \\ 0 & 0 & k_{3333} \end{pmatrix}$. One better also takes the other stresses into account and investigates their possible influence regarding the resulting global wear, which, in this case, has to be taken as the sum over all stress-components in connection with the wear-tensor

$$h_w = k_{33kl}\ \sigma^{kl} = k_{3311}\sigma^{11} + k_{3322}\sigma^{22} + k_{3333}\sigma^{33} + 2\left(k_{3312}\sigma^{12} + k_{3313}\sigma^{13} + k_{3323}\sigma^{23}\right) \qquad (24)$$

Here we have made use of the symmetry of the stress tensor, also requiring a symmetric wear-tensor.

Even though, in principle, we have now said what is of need, we explicitly point out again, that wear cannot be connected by a simple k_d-value (simple Archard's law) to the deformation or stress field. Instead, in the most simple cases, the wear is a tensor, coupling with wear-moduli or wear-components to every stress component in a fully covariant manner:

$$w_{ij} = k_{ijkl}\ \sigma^{kl} \qquad (25)$$

We also point out, that in the general law as given above the hydrostatic (sphere) and deviatoric stress parts are distinguishable. Such a simplified law might read:

$$w_{ij} = \delta_{ij}\left(k_{dM}\sigma_M + k_{dH}\sigma_H + k_{ll}\sigma^{ll}\right) \qquad (26)$$

With σ_M, σ_H denoting the von Mises and the hydrostatic stress, respectively.

The Procedure and Results

Now we need to connect the various models and concepts introduced and elaborated above in order to construct a compact optimization circle including wear test and simulation.

This shall be illustrated by the means of a practical example for cutting tools as follows:

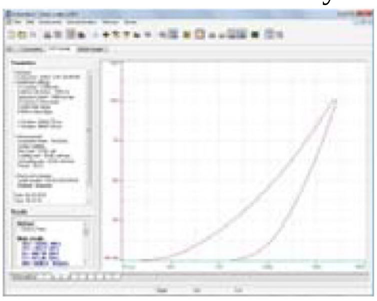
Step 1

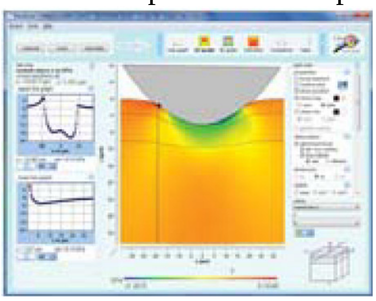
Step 2

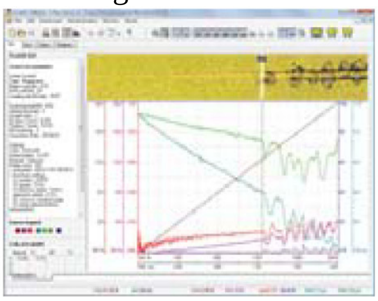
Step 3

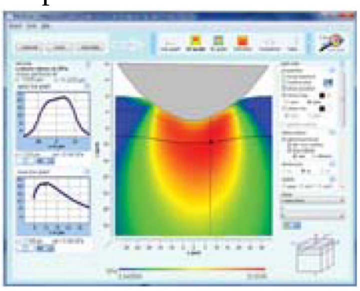
Step 4

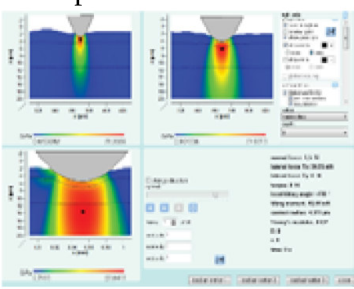
Step 5

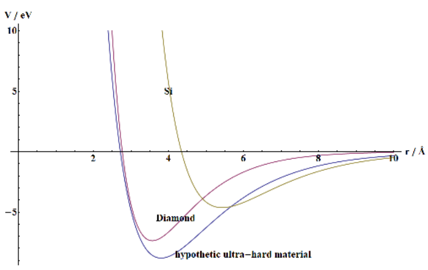

Step 6

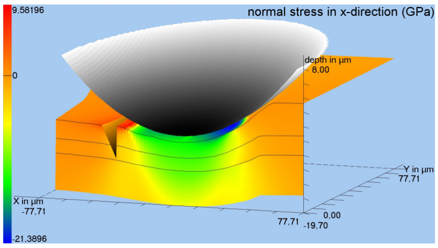

Step 7

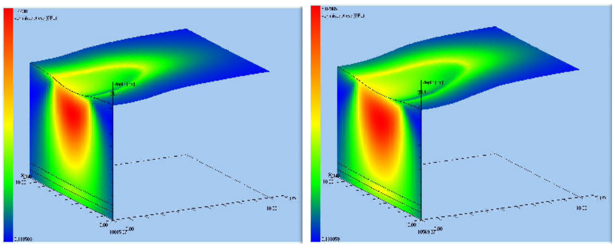
Step 8 (from middle of wear test to its end)

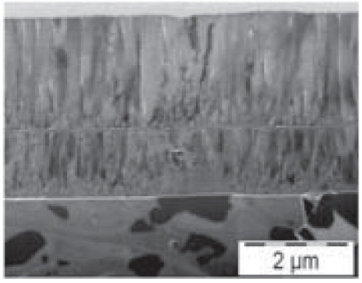

Step 9 (*reproduced from [46], with permission of the authors*)

Step 1:
Nanoindentation tests are performed to accurately measure the materials properties of the substrate and coatings, taking into account possible property profiles [38, 39].

Step 2:
With the mechanical properties previously measured by nanoindentation, a calculation of the stress-strain fields of a simulated scratch allows a perfect dimensioning of the scratch test [29, 30].

Step 3:
Scratch testing with the defined conditions is performed.

Step 4:
An advanced analysis with integration of the residual penetration depth, pre-scan surface profile, and friction coefficient is made with the simulation software in order to perfectly know the stress-strain field [24].

Step 5:
For better understanding, an animation of the scratch is created (examples under: www.siomec.de/en/096/Examples).

Step 6:
From the results of the previous steps effective interatomic potentials are evaluated and decomposition parameters are derived as shown in [5]. These parameters are used to design a tribo-test optimum for the later application in question.

Step 7:
Performance of tribo-test as designed in step 6 and analysis by inversed global increment wear model [9] improved with layered half space model and extended Hertzian approach.

Step 8:
For better understanding, an animation of the tribo- resp. wear-test is created (c.f. figures 7 - 15 below).

Step 9:
Optimization of coating-substrate system. Going to next circle.

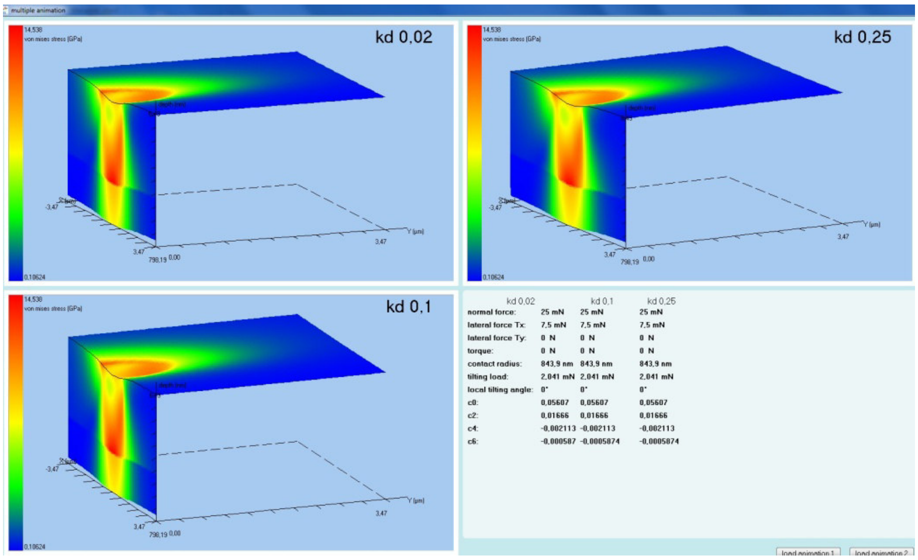

Fig. 7: Wear track evaluation of an oscillating pin (linear wear track) on three different coating materials. Beginning of the Wear test. Von Mises stress.

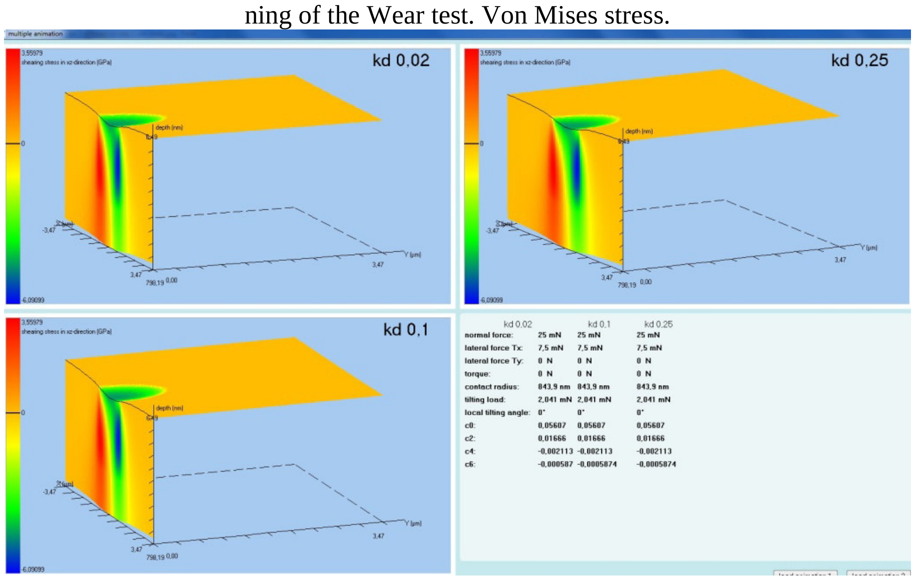

Fig. 8: Wear track evaluation of an oscillating pin (linear wear track) on three different coating materials. Beginning of the Wear test. Shear stress in normal-lateral direction.

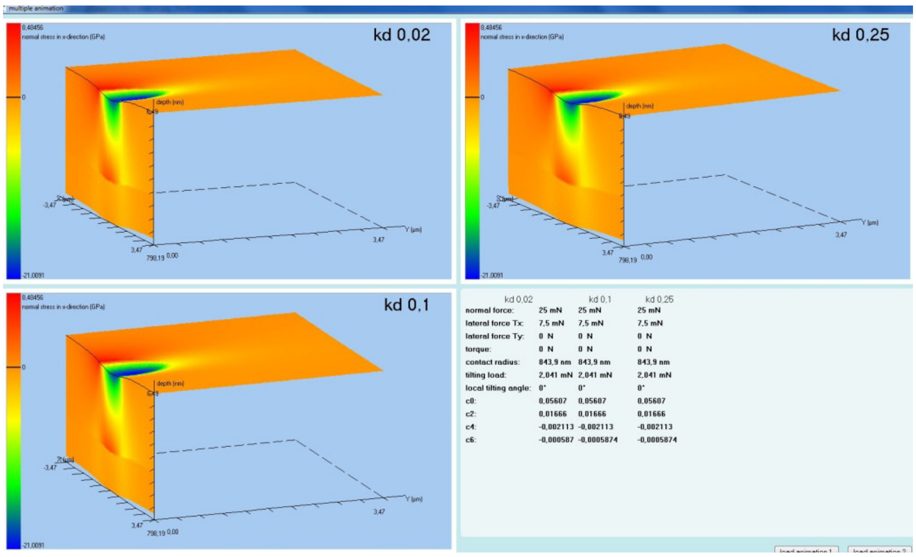

Fig. 9: Wear track evaluation of an oscillating pin (linear wear track) on three different coating materials. Beginning of the Wear test. Normal lateral stress in direction of the moving pin.

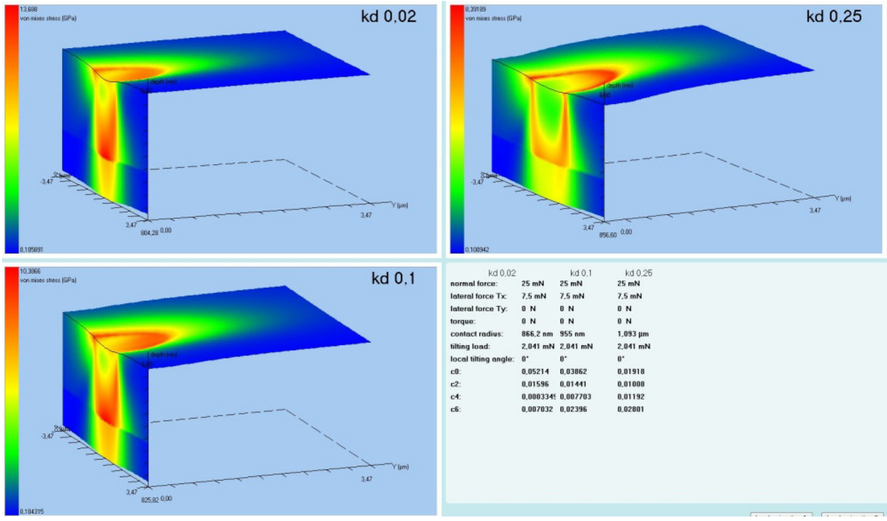

Fig. 10: Wear track evaluation of an oscillating pin (linear wear track) on three different coating materials. Middle of the Wear test. Von Mises stress.

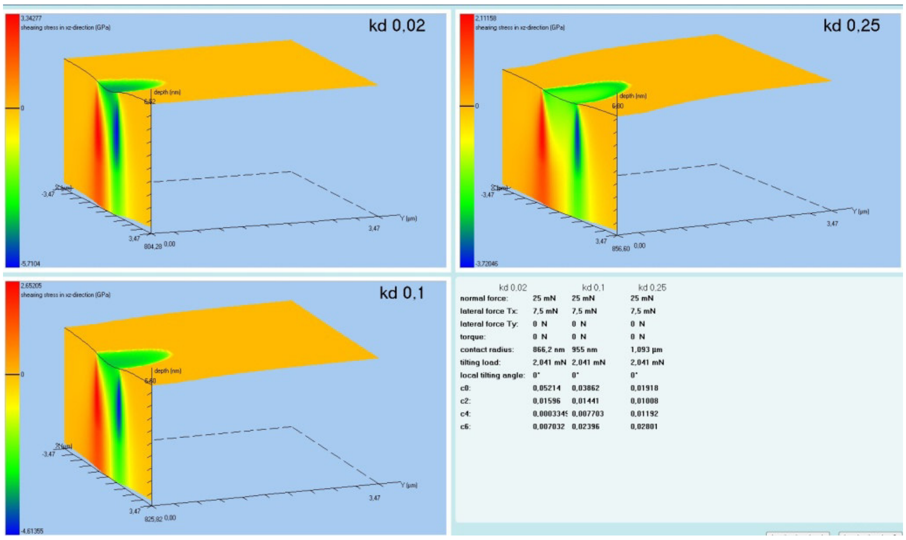

Fig. 11: Wear track evaluation of an oscillating pin (linear wear track) on three different coating materials. Middle of the Wear test. Shear stress in normal-lateral direction.

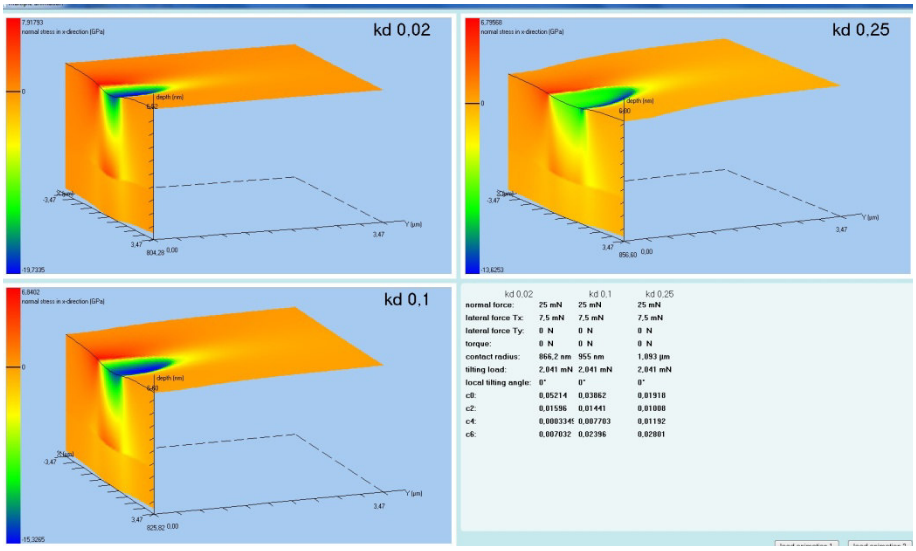

Fig. 12: Wear track evaluation of an oscillating pin (linear wear track) on three different coating materials. Middle Beginning of the Wear test. Normal lateral stress in direction of the moving pin.

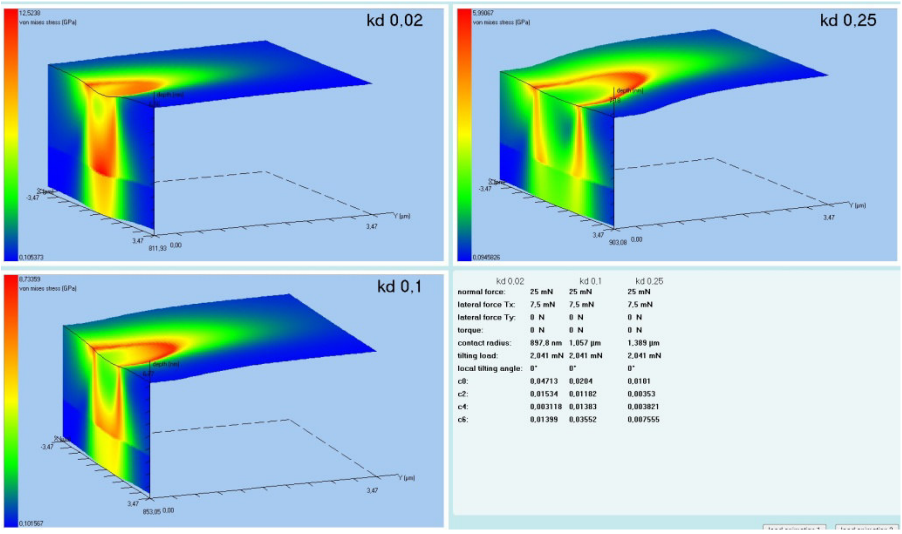

Fig. 13: Wear track evaluation of an oscillating pin (linear wear track) on three different coating materials. End of the Wear test. Von Mises stress.

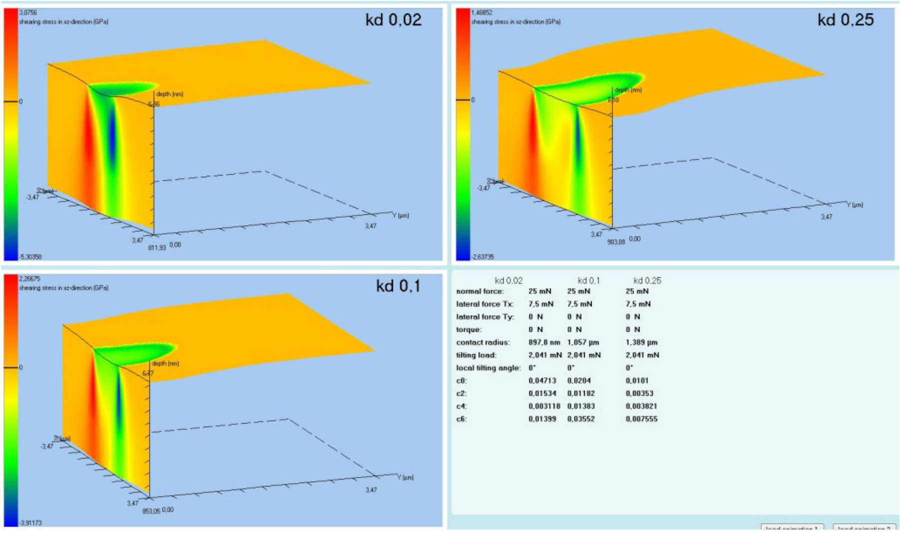

Fig. 14: Wear track evaluation of an oscillating pin (linear wear track) on three different coating materials. End of the Wear test. Shear stress in normal-lateral direction.

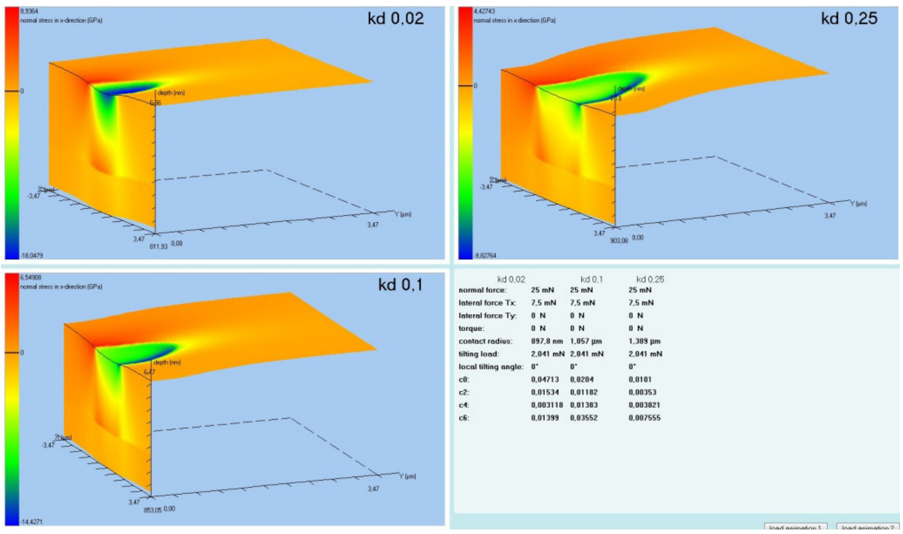

Fig. 15: Wear track evaluation of an oscillating pin (linear wear track) on three different coating materials. End of the Wear test. Normal lateral stress in direction of the moving pin.

Examples

The method was applied, sometimes in parts sometimes completely, to a variety of examples which are published elsewhere (e.g. [29, 30] and [41 – 45]).

Conclusions

By combining the global increment wear model with the concept of the effective indenter, the extended Hertzian approach and a layered half space solution for contact problems with rather arbitrary combinations of normal, lateral and tilting loads a general, quick and powerful wear model has been created.
Inversion of the model makes it fit for parameter identification problems.
Further adding first principle models, like effective interatomic interaction potentials allows a deeper understanding of those failure mechanisms being responsible for wear results observable in practical tests.

Acknowledgements

This work was partially funded through the European Metrology Research Programme (EMRP) Project IND05 MeProVisc. The EMRP is jointly funded by the EMRP participating countries within EURAMET and the European Union.

References

[1] N. Schwarzer, Short note on the effect of pressure induced increase of Young's modulus, Philosophical Magazine, accepted January 2012, vol. 92, issue 13, pp. 1631-1648
[2] N. Schwarzer, G. M. Pharr: „On the evaluation of stresses during nanoindentation with sharp indenters", Thin Solid Films, Vol. 469-470C pp. 194-200
[3] N. Schwarzer, T. Chudoba, G. M. Pharr: „On the evaluation of stresses for coated materials during nanoindentation with sharp indenters", Surf. Coat. Technol, Vol 200/14-15 pp 4220-4226
[4] N. Schwarzer: "The extended Hertzian theory and its uses in analysing indentation experiments", Phil. Mag. 86(33-35) 21 Nov - 11 Dec 2006 5153 – 5767, Special Issue: "Instrumented Indentation Testing in Materials Research and Development"
[5] N. Schwarzer, "Is ultra-hardness possible - a brief feasibility study", www.siomec.de/ultra-hard-coatings, also invited for publication in Phil. Mag.
[6] M. Lie, N. X. Chen, Möbius inversion transform for diamond-type materials and phonon dispersions, Physical Review B, 52, No. 2 (1995), 997 - 1003
[7] T. Dick, G. Cailletaud, (2006) Computational Materials Science, 38, 113-125
[8] J. M. Guilemany, S. Dosta, J. R. Miguel, (2006) Surface and Coatings Technology 201, 1180-1190
[9] V. Hegadekatte, N. Huber, O. Kraft, (2006) Tribology Letters 24, 51-60
[10] R. Holm, (1946) Electric contacts , Almqvist and Wiksells Boktryxkeri AB, Uppsala
[11] K. Holmberg, A. Matthews, (2009) Coatings Tribology. 2nd edition, Springer, Amsterdam, The Netherlands
[12] A. Bolshakov, W.C. Oliver, and G.M. Pharr, MRS Symp. Proc 356, p 675 (1995)
[13] Pharr GM, Bolshakov B (2002) Understanding nanoindentation unloading curves, J. Mater. Res., Vol. 17, No. 10, Oct 2002
[14] N. Schwarzer: "Arbitrary load distribution on a layered half space", ASME Journal of Tribology, Vol. 122, No. 4, October 2000, 672 - 681
[15] W. C. Oliver, G. M. Pharr, An improved technique for determining hardness and elastic modulus using load and displacement sensing indentation experiments, J. Mat. Res. 7 (1992) 1564-1583.

[16] T. Chudoba, K. Herrmann, Härtereitechnische Mitteilungen, HTM 56 (2001) 258
[17] N. Schwarzer, J. Phys. D: Appl. Phys., 37 (2004) 2761-2772
[18] N. Schwarzer, G. M. Pharr, Thin Solid Films, Vol. 469-470C pp. 194-200
[19] N. Schwarzer, T. Chudoba, G. M. Pharr, Surf. Coat. Technol, Vol. 200/14-15 pp 4220-4226
[20] N. Schwarzer, T. Chudoba, F. Richter, Surf. Coat. Technol., Vol 200/18-19 pp 5566-5580
[21] N. Schwarzer, Thin Solid Films 494 (2006) 168 – 172
[22] N. Schwarzer, Phil. Mag. 86(33-35) 21 Nov - 11 Dec 2006 5153 – 5767
[23] R. Puschmann, N. Schwarzer, F. Richter, S. Frühauf, S. E. Schulz: “An applicable concept for the indentation of thin porous films”, proceedings of the NanoMech 5, 7-9 September 2004 in Hückelhoven, Germany, also in Z. Metallkd. 96 (2005) 11, 1-6
[24] FilmDoctor: Software demonstration package, www.siomec.de/FilmDoctor
[25] A.C. Fischer-Cripps, A simple phenomenological approach to nanoindentation creep, Materials Science and Engineering A 385 (2004) 74–82
[26] D. François, A. Pineau, A. Zaoui, Mechanical Behaviour of Materials, Kluwer Academic Publishers, The Netherlands, 1998
[27] ISO 20502 Fine ceramics (advanced ceramics -advanced technical ceramics) - Determination of adhesion of ceramic coatings by scratch testing
[28] ASTM C1624 Standard Test Method for Adhesion Strength and Mechanical Failure Modes of Ceramic Coatings by Quantitative Single Point SCRATCH Testing
[29] M. Fuchs, G. Favaro, " Physical characterization of coated surfaces, Part II: Scratch Test", Application Bulletin No. 38 of CSM instruments, free download at: www.csm-instruments.com/en/Physical-characterization-of-coated-surfaces-Part-II-%3A-Scratch-Test
[30] N. Schwarzer, Q.-H. Duong, N. Bierwisch, G. Favaro, M. Fuchs, P. Kempe, B. Widrig, J. Ramm, Optimization of the Scratch Test for Specific Coating Designs, Surface and Coatings Technology, volume 206, issue 6, year 2011, pp. 1327 - 1335
[31] N. Schwarzer, (2007) “Intrinsic stresses – Their influence on the yield strength and their measurement via nanoindentation", online archives of the Saxonian Institute of Surface Mechanics www.siomec.de/pub/2007/001
[32] N. Schwarzer, "Modelling of Contact Problems of Rough Surfaces", online archives of the Saxonian Institute of Surface Mechanics www.siomec.de/pub/2007/007
[33] N. Schwarzer, Some Basic Equations for the Next Generation of Surface Testers Solving the Problem of Pile-up, Sink-in and Making Area-Function-Calibration obsolete, JMR Special Focus Issue on “Indentation Methods in Advanced Materials Research”, J. Mater. Res., Vol. 24, No. 3, March 2009, 1032 - 1036
[34] N. Schwarzer, Basic Equations for the Next Generation of Surface Testers for the Case of an Elastic Indenter and a Layered Samples, online archive of the Saxionian Institute of Surface Mechanics, www.siomec.de/pub/2008/001
[35] N. Schwarzer: Analyse und Simulation der mechanischen Eigenschaften beschichteter Polymere unter Berücksichtigung der meist zeitabhängigen Materialparameter, 19. NDVaK, 19. u. 20.10. 2011 Dresden, Germany, ISBN 978-3-9812550-3-4, pp. 96 - 101
[36] J.G. Kohl, N.X. Randall, N. Schwarzer, T.T. Ngo, J.M. Shockley, and R.P. Nair, "An Investigation of Scratch Testing of Silicone Elastomer Coatings with a Thickness Gradient", Journal of Applied Polymer Science, Vol. 124, 2978–2986 (2012), pp. 2978-2986
[37] N. Schwarzer, "Determination of storage and loss modulus from quasi-static nanoindentation experiments", submitted to Phil. Mag. September 2012

[38] V. Linss, N. Schwarzer, T. Chudoba, M. Karniychuk, F. Richter: “Mechanical Properties of a Graded BCN Sputtered Coating with VaryingYoung's Modulus: Deposition, Theoretical Modelling and Nanoindentation”, Surf. Coat. Technol., 195 (2005) pp 287 - 297

[39] T. Chudoba, N. Schwarzer, V. Linss, F. Richter: „Determination of Mechanical Properties of Graded Coatings using Nanoindentation”, proceedings of the ICMCTF 2004 in San Diego, California, USA, also in Thin Solid Films (2004): 469-470C pp. 239-247

[40] N. Schwarzer: „Modelling of the mechanics of thin films using analytical linear elastic approaches“, Habilitationsschrift der TU-Chemnitz 2004, FB Physik Fester Körper, www.*siomec*.de/pub/2007/001

[41] T. Chudoba, N. Schwarzer, A. Gies: „3D micro scratch tests in combination with a comprehensive stress analysis – a new tool for the understanding of surface failures“ submitted as oral presentation for ICMCTF 2013, will also be submitted for the ICMCTF-proceedings

[42] A. Gies, T. Chudoba, N. Schwarzer, J. Becker: „Influence of the coating structure of a-C:H-W coatings on their wear-performance: a theoretical approach and its practical confirmation“, submitted as oral presentation for ICMCTF 2013, will also be submitted for the ICMCTF-proceedings

[43] N. Bierwisch, N. Schwarzer, El Seweifi, M. Griepentrog, P. Reinstädt: „Examples for the time dependent effective indenter concept“, submitted as poster presentation for ICMCTF 2013, will also be submitted for the ICMCTF-proceedings

[44] N. Schwarzer: “How to Make Tribological Tests Physical?”, submitted as oral presentation, for ICMCTF 2013, will also be submitted for the ICMCTF-proceedings

[45] Florian Seibert, Max Döbeli, Doris M. Fopp-Spori, Kerstin Glaentz, Helmut Rudigier, Norbert Schwarzer, Beno Widrig, Jürgen Ramm, Comparison of arc evaporated Mo-based coatings versus Cr1N1 and ta-C coatings by reciprocating wear test, wear, submitted February 2012, accepted October 2012

[46] E. Bemporad, M. Sebastiani, M.H. Staia, E. Puchi Cabrera, Tribological studies on PVD/HVOF duplex coatings on Ti6Al4V substrate, Surface & Coatings Technology 203 (2008) 566–571